AhR activation defends gut barrier integrity against damage occurring in obesity

Bárbara G. Postal [1,2,7,8], Sara Ghezzal [1,8], Doriane Aguanno [1,2,3], Sébastien André [4], Kevin Garbin [5], Laurent Genser [4], Edith Brot-Laroche [1], Christine Poitou [4,6], Hédi Soula [4], Armelle Leturque [1,4], Karine Clément [4,6], Véronique Carrière [1,2,*,7]

ABSTRACT

Objective: Obesity is characterized by systemic and low-grade tissue inflammation. In the intestine, alteration of the intestinal barrier and accumulation of inflammatory cells in the epithelium are important contributors of gut inflammation. Recent studies demonstrated the role of the aryl hydrocarbon receptor (AhR) in the maintenance of immune cells at mucosal barrier sites. A wide range of ligands of external and local origin can activate this receptor. We studied the causal relationship between AhR activation and gut inflammation in obesity.

Methods: Jejunum samples from subjects with normal weight and severe obesity were phenotyped according to T lymphocyte infiltration in the epithelium from lamina propria and assayed for the mRNA level of AhR target genes. The effect of an AhR agonist was studied in mice and Caco-2/TC7 cells. AhR target gene expression, permeability to small molecules and ions, and location of cell-cell junction proteins were recorded under conditions of altered intestinal permeability.

Results: We showed that a low AhR tone correlated with a high inflammatory score in the intestinal epithelium in severe human obesity. Moreover, AhR activation protected junctional complexes in the intestinal epithelium in mice challenged by an oral lipid load. AhR ligands prevented chemically induced damage to barrier integrity and cytokine expression in Caco-2/TC7 cells. The PKC and p38MAPK signaling pathways were involved in this AhR action.

Conclusions: The results of these series of human, mouse, and cell culture experiments demonstrate the protective effect of AhR activation in the intestine targeting particularly tight junctions and cytokine expression. We propose that AhR constitutes a valuable target to protect intestinal functions in metabolic diseases, which can be achieved in the future via food or drug ligands.

1. INTRODUCTION

The development of obesity is characterized by a progressive aggravation of systemic low-grade inflammation together with metabolic deterioration. Inflammation in obese subjects also occurs in the adipose tissue [1,2], liver [3], and small intestine [4]. During obesity, adipose tissue directly contributes to inflammation in the systemic vascular system and, when accumulated in the visceral depot, through the portal vein via the release of free fatty acids, cytokines, and adipokines [5]. Recent reports highlighted the intestine's role as an early contributor to low-grade inflammation. Studies in mouse models of high-fat diet-induced obesity suggested that the passage of bacterial components such as lipopolysaccharides (LPS) from the intestinal lumen into the circulation promotes systemic inflammation through mechanisms involving intestinal barrier damage [6—8]. Intestinal permeability increased during the first week of a high-fat diet in mice [9,10] and, as we recently demonstrated, after a single gavage with palm oil [11]. The latter results suggested that intestinal barrier defects might precede the onset of obesity. In humans, we showed that the higher accumulation of T lymphocyte density in the jejunal epithelium of obese patients compared to non-obese subjects was associated with markers of systemic inflammation [4]. In the fasting state, subtle alterations of the intestinal barrier were evidenced in jejunum samples of subjects with severe obesity and these alterations were further enhanced after an *ex-vivo* lipid challenge [12]. Patient susceptibility to lipid-induced barrier defects correlated with both intestinal and

[1]Cordeliers Research Center, Sorbonne University, Paris Dauphine University 05, INSERM, CNRS, F-75006, Paris, France [2]Saint-Antoine Research Center, Sorbonne University, INSERM, F-75012, Paris, France [3]EPHE, PSL Research University, F-75006, Paris, France [4]Sorbonne University, INSERM, NutriOmics Research Unit Paris, F-75013, France [5]CHIC Platform of Cordeliers Research Center, Sorbonne University, UPD Univ Paris 05, INSERM, F-75006, Paris, France [6]Assistance Publique-Hôpitaux de Paris, Pitié-Salpêtrière Hospital, Nutrition Department, CRNH Ile de France, F-75013, Paris, France

[7] Present address: Saint-Antoine Research Center, Sorbonne University, INSERM, Paris F-75012 France.
[8] Bárbara G. Postal and Sara Ghezzal contributed equally to this work.

*Corresponding author. Véronique Carrière, Center de Recherche Saint-Antoine, UMRS 938, Equipe P. Seksik and H. Sokol, 27 Rue de Chaligny, Paris, F-75012, France. Tel.: +33 1 40 01 13 89. E-mail: veronique.carriere@sorbonne-universite.fr (V. Carrière).

Abbreviations: βNF, β-naphthoflavone; DDT, dithiothreitol; FCS, fetal calf serum; FITC-dextran, fluorescein isothiocyanate-dextran

Original Article

systemic inflammation. Altogether, these studies established a link between the intestinal barrier and low-grade inflammation in obesity, and the molecular factors that orchestrate this relationship must be deciphered.

Data highlight the role of AhR in metabolic diseases and inflammation. Aryl hydrocarbon receptor (AhR), a transcriptional factor acting as an environmental chemical sensor, was first extensively studied for its role in the metabolism of xenobiotics [13,14]. Investigations using AhR knockout mouse models demonstrated its important role in the development and control of the immune system [15]. In the gut, a protective role of AhR in inflammation or barrier injury has been reported. It seems to be related to its role in the differentiation of intraepithelial lymphocytes and modulation of innate lymphoid cells [15]. In humans, a loss of protective AhR function was proposed to occur in intestinal bowel diseases, which were linked to the reduced production of AhR agonists by individual gut microbiota [16]. A beneficial effect of AhR agonists on the intestinal barrier in mouse models or intestinal cells submitted to inflammatory stresses has been reported [17,18]. In metabolic diseases, contradictory results were obtained concerning the importance of AhR tone. Recent reports showed that AhR-deficient mice were protected from diet-induced obesity and associated metabolic disorders such as insulin-resistance and hepatic steatosis [19,20]. Conversely, the activation of AhR using genetic mouse models or specific ligands such as TCDD promoted hepatic steatosis [21,22]. This deleterious impact of AhR activation is in contrast with the reported protective role of AhR in liver steatosis in mice [23,24]. Moreover, in humans, low levels of AhR agonists in the feces were associated with metabolic syndrome, type 2 diabetes, increased body mass index, and high blood pressure [24].

Combining a series of human studies, in vivo mouse models, and in vitro analyses, we aimed to determine the potential implication of AhR in intestinal inflammation and barrier dysfunction reported in obesity.

2. MATERIALS AND METHODS

2.1. Human subjects' clinical and biological characteristics
This study is ancillary to two previously published studies [12,25] that included populations of patients with severe obesity in a bariatric surgery program (Roux-en-Y gastric bypass) at Pitié-Salpêtrière

University Hospital, Nutrition and Visceral Surgery Departments, Paris, France. Non-obese subjects underwent pancreaticoduodenectomy or gastrectomy allowing access to proximal jejunal samples. For this study purpose, a subgroup of 36 subjects including 26 severely obese and 10 non-obese subjects was selected free of diabetes based on international definitions and with no personal or familial history of inflammatory bowel disease. Their white blood count levels were under 10.109/mm3 and CRP levels were under 5 mg/l. We excluded non-obese subjects with renal, cardiac, or hepatic failure. This study was conducted in accordance with the Declaration of Helsinki, received approval from the local ethics committee (CPP Ile de France I), and was registered as number NCT02292121 on the ClinicalTrials.gov website. Informed written consent was obtained from patients prior to study inclusion. Medical history and clinical variables were recorded for non-obese and obese patients before surgery as described in [12]. Venous blood samples were collected after a 12-h fast for the routine assessment of biological metabolism as previously described [26]. Insulin resistance was assessed using the HOMA-IR index (insulinemia [mIU/L] x fasting blood glucose [mmol/L]/22.5). The clinical characteristics of the non-obese and severely obese patients included in this study are provided in Table 1. Due to the unequal gender distribution between our control and obese groups and to avoid experimental bias, correlations between AhR/AhR target genes and CD3+ T lymphocytes were assessed only in the obese group and only with female subjects.

2.2. Human jejunum tissue sampling, epithelium cell preparation, and analyses
Proximal jejunum samples from obese subjects and non-obese subjects were collected during surgery, conditioned, and transported as described [4]. Briefly, proximal jejunal samples (60−70 cm distal to the ligament of Treitz) were collected from surgical waste (4 cm). Tissue was rapidly opened, washed in DMEM (1 g GlutaMAX glucose + pyruvate + 10% SVF + 1% penicillin/streptomycin), and maintained at 4 °C before cell isolation, fixation, and paraffin imbedding or freezing at −80 °C.

Immunohistology of the jejunum (5 μm paraffin-embedded tissue sections) was conducted using anti-CD3 polyclonal antibody (A0452, DAKO, Agilent Technologies, Les Ulis, France). Primary or secondary antibody were incubated for 1 h at room temperature and revealed with a streptavidin biotin peroxidase kit (GMR4-61, BioSpa Milan, Italy), DAB

Table 1 — Clinical and biological baseline characteristics of nonobese and obese patients enrolled in the study			
	nonobese (n= 10)	obese (n= 26)	p value obese vs nonobese
Demographic data			
sex ratio M/F, %	100/0	4/96	<0.0001
age (years)	58.8 ± 4.9 (42−84)	39.3 ± 2.3 (21−64)	0.0002
Corpulence and adiposity			
weight (kg), mean ± SEM (min−max)	69.5 ± 3.2 (50−87)	124.3 ± 4.7 (83.1−184.4)	<0.0001
BMI (kg/m2), mean ± SEM (min−max)	22.6 ± 0.82 (16.9−26.37)	46.5 ± 1.3 (38.1−56.9)	<0.0001
Comorbidities			
type 2 diabetes, %	0	0	—
dyslipidemia, %	16	90	0.0164
hypertension, %	0	25	0.1310
Glucose metabolism			
glycemia (mmol/L), mean ± SEM (min−max)	—	5.3 ± 0.1 (4.3−6.4)	—
insulinemia (mU/L), mean ± SEM (min−max)	—	25.1 ± 3.9 (9.5−67.5)	—
HOMA-IR index, mean ± SEM (min−max)	—	6.3 ± 1.1 (2.4−18.7)	—
Lipid metabolism			
total cholesterol (mmol/L), mean ± SEM (min−max)	—	5.0 ± 0.2 (3.3−7.2)	—
triglycerides (mmol/L), mean ± SEM (min−max)	—	1.3 ± 0.08 (0.47−1.96)	—
HDL (mmol/L), mean ± SEM (min−max)	—	1.1 ± 0.06 (0.7−1.6)	—
LDL (mmol/L), mean ± SEM (min−max)	—	3.3 ± 0.2 (1.9−5.2)	—

staining (DAKO, Agilent Technologies), and nuclei hematoxylin counterstaining (Vector, Eurobio, Les Ulis, France). Images were obtained by conventional microscopy. Lamina propria and epithelial immune cell densities (cell/mm^2) excluding lymphoid structures were analyzed in longitudinal sections of mucosa in two to four fields (ImageJ 1.46c). Epithelial cell fractions from the intestinal mucosa were prepared as described in [4]. Briefly, the jejunal mucosa was dissected and minced prior to incubation in chelating buffer (5 mM EDTA, 2 mM DDT, and PBS at 37°C for 20 min). Released epithelial cells were filtered through 70 µm mesh cell strainers, centrifuged (600 g at 4°C for 5 min), and recovered in complete DMEM (10% FCS, 1% penicillin/streptomycin). Total RNA was extracted from epithelial fractions with an RNAeasy Mini kit (QIAGEN, Thermo Fisher Scientific, Illkirch, France). The RNA concentration and quality were assessed (2100 Bioanalyzer, Agilent Technologies) before reverse transcription of total RNA (Applied Biosystems, Thermo Fisher Scientific). qPCR analyses were conducted using TaqMan Low-Density Arrays (Thermo Fisher Scientific) according to the manufacturer's procedures with the following gene assay IDs: AhR (Hs00907314_m1), AhRR (Hs01005075_m1), CYP1A1 (Hs01054797_g1), CYP1B1 (Hs00164383_m1), and IL22 (Hs01574154_m1). The results were normalized to the geometric mean of ribosomal 18S (Hs99999901_s1) and peptidylprolyl isomerase B (cyclophilin B, Hs00168719_m1) values.

2.3. Mouse treatments and *in vivo* intestinal permeability
Three-month-old male C57BL/6JRj mice (Janvier Labs, Le Genest-Saint-Isle, France) were fed a standard chow diet *ad libitum* (A03, SAFE, Augy, France) during the experiments. The mice were housed under an artificial light—dark cycle 12:12 h with lights on at 07:00 am. The mice were force fed 0.2 ml of water, palm oil (Sigma—Aldrich, Saint Quentin-Fallavier, France), or βNF (40 mg/kg, Sigma—Aldrich) dissolved in palm oil for 4 consecutive days at 6:00 pm just before the feeding period. For *in vivo* intestinal permeability measurements, the mice were successively force fed on the fifth day of the experiment 0.2 ml of palm oil or βNF dissolved in palm oil followed by 0.2 ml of 4 kDa FITC-dextran solution (Sigma—Aldrich, 0.5 mg/g in water) at 9:00. No significant change in the weight of the animals was observed whatever the treatment. The mice were anesthetized and then euthanized 1 h after the last gavage. Blood and jejunum were collected. The FITC-dextran concentrations were determined in the plasma by fluorometry (FLUOstar Omega, BMG Labtech, Champigny-sur-Marne, France). All of the mice experiments were approved by the French Ministry of Education and Research and Animal Care and Use Committee No. 5 (agreement number: APAFIS#2710-201510301447819).

2.4. Cell culture, cell treatments, and cytotoxicity assay
The Caco-2/TC7 cell line is a clonal population of human colon carcinoma-derived Caco-2 cells that reproduces to a high degree most of the morphological and functional characteristics of normal human absorptive enterocytes [27]. The cells were assessed for the absence of mycoplasma contamination. In all of the experiments, the cells were cultured in 6-well Transwell filters (Thermo Fisher Scientific) for 3 weeks to obtain fully differentiated enterocyte-like cells as previously described [28,29]. The cells were treated with 20 µM βNF added in both the apical and basal compartments. In some experiments, the cells were treated with 4.5 mM EGTA (Sigma—Aldrich, St. Quentin Fallavier, France) added in the upper compartment. The duration of treatments is indicated in the figure legends. In some experiments, the cells were pre-incubated with 5 µM of protein kinase C inhibitor Ro 31-8220 (Calbiochem, Merck Chimie, Fontenay-sous-Bois, France) or

10 µM of ERK1/2 protein inhibitor U0126 (Cell Signaling, Ozyme, Saint-Cyr-l'École, France) or 20 µM of p38MAPK inhibitor SB203580 (5633S, Calbiochem, Merck Chimie, France), 1 h prior to βNF addition. These treatments were repeated daily for 4 days. The protein kinases inhibitors were added to both the upper and lower compartments of the filters. At the end of the experiment, the cytotoxicity of the treatments was evaluated by measuring the lactate dehydrogenase activity in apical medium according to the manufacturer's instructions (Cytotoxicity Detection KitPLUS, Sigma—Aldrich, St. Quentin Fallavier, France).

2.5. Permeability and transepithelial electrical resistance (TEER) measurements in Caco-2/TC7 cells
To assess paracellular permeability, 1 mg/ml of 4 kDa FITC-dextran (TdB Consultancy AB, Uppsala, Sweden) was added to the apical medium on the last day of treatment. Samples of basal medium were collected after 4 h, and fluorescence was determined with a microplate fluorometer (FLUOstar Omega; BMG Labtech, Champigny s/Marne, France). Transepithelial electrical resistance (TEER), which is inversely proportional to ion permeability, was measured before and after treatments using a volt-ohm meter (Millipore, Guyancourt, France).

2.6. Total RNA extraction and RT-PCR analysis
Total RNA from the Caco-2/TC7 cells was extracted with TRI Reagent (Molecular Research Center, Cincinnati, OH, USA) according to the manufacturer's instructions. Reverse transcription (RT) was conducted with 1 µg of RNA using a high-capacity cDNA reverse transcriptase kit (Applied Biosystems, Thermo Fisher Scientific). Semi-quantitative real-time polymerase chain reactions were performed with the Mx3000P Stratagen system using SYBR Green (Agilent, Les Ulis, France) according to the manufacturer's procedures. The human primer sequences were 5′-AGACAGCAGAGCACACAAGC-3′ forward and 5′-ATGGTTCCTTCCGGTGGT-3′ reverse for CXCL8 (IL-8), 5′-CTGTCCTGCGTGTTGAAAGA-3′ forward and 5′-TTGGGTAATTTTTGG-GATCTACA-3′ reverse for IL1B (IL1-β), 5′-CAGCCTCTTCTCCTTCCTGA-3′ forward and 5′-GCCAGAGGGCTGATTAGAGA-3′ reverse for TNFA, and 5′-TCCAAGAGTCCACCCTTCC-3′ forward and 5′-AAGCATGAT-CAGTGTAGGGATCT-3′ reverse for CYP1A1. PPIB (cyclophilin B) gene was used as a reference gene. The primer sequences were 5′-GCCTTAGCTACAGGAGAGAA-3′ forward and 5′-TTTCCTCCTGTGCCATCTC-3′ reverse.

2.7. Cytokine secretion
The cytokine IL-8 protein level was quantified in basal medium (0.2 ml) of Caco-2/TC7 cells by enzyme-linked immunosorbent assay (ELISA) using a kit from R&D Systems (Lille, France).

2.8. Analysis of junctional proteins by immunofluorescence
Immunofluorescence analyses were conducted as previously described [30]. Briefly, Caco-2/TC7 cells were fixed and permeabilized by incubation for 5 min in methanol at −20 °C. For immunostaining on these cells, we used primary antibodies for tricellulin (1:200, MAR-VELD2 700191, Thermo Fisher Scientific), ZO-1 (1:200, ZO1-1A12, 33-9100 Thermo Fisher Scientific), and occludin (1:200, 71-1500, Thermo Fisher Scientific). Jejunum cryosections were fixed for 30 min with 4% paraformaldehyde at 4 °C and permeabilized for 30 min in 0.1% Triton X-100 at 4 °C. For immunostaining of mouse jejunum cryosections, we used primary antibodies for tricellulin (1:10, Tric2469, kindly provided by Dr. Furuse [31,32]), ZO-1 (1:200, 617300, Thermo Fisher Scientific), and occludin (1:10, Moc-37, kindly provided by Dr. Furuse [33]). Alexa 488- and Alexa 546-conjugated anti-immunoglobulin G were used as secondary antibodies (1:400,
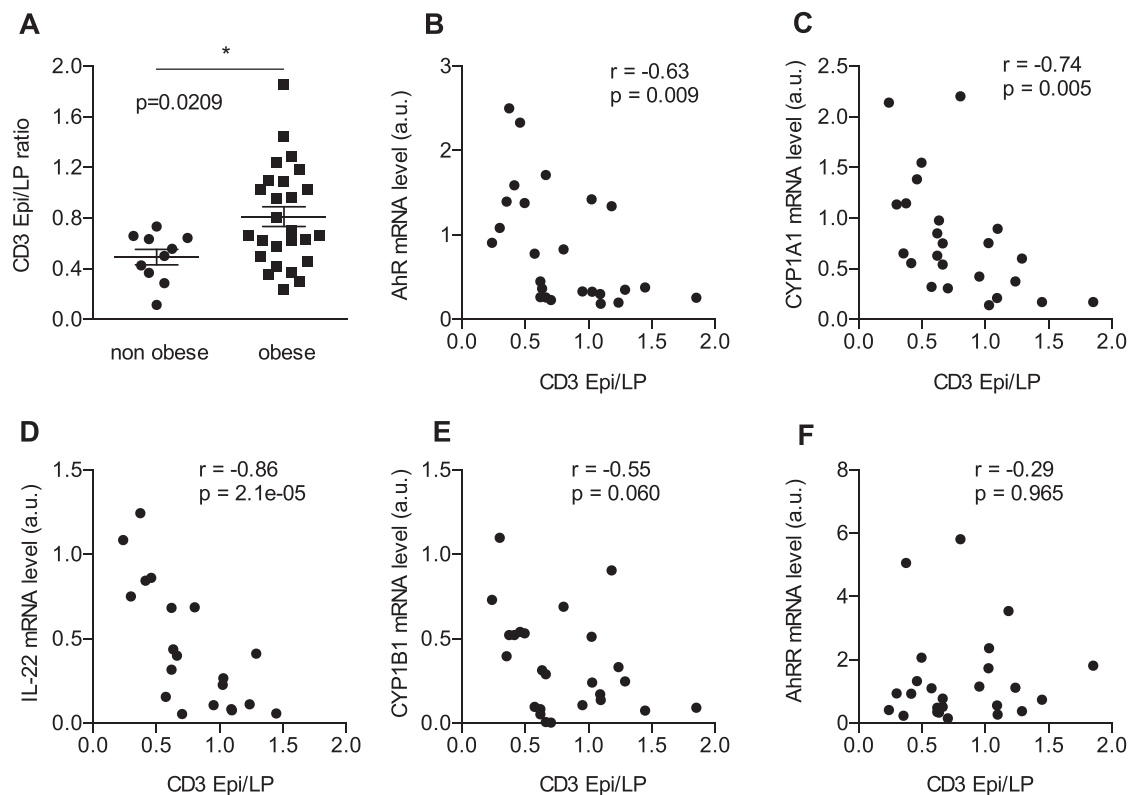
Figure 1: Low expression of AhR target genes in obese subjects with intestinal inflammation. (**A**) $CD3^+$ T cell density (cell/mm^2) in the epithelium/lamina propria ratio (Epi/LP) was determined by immunohistochemistry in the jejunum of non-obese (n = 10) and obese subjects (n = 26). The results are expressed as mean ± SEM, *p < 0.05. (**B**–**F**) Pearson's correlations of AhR (**B**), CYP1A1 (**C**), IL-22 (**D**), CYP1B1 (**E**), AhRR, and (**F**) mRNA levels in the intestinal epithelium and CD3 Epi/LP ratios in female obese subjects. AhR: aryl hydrocarbon receptor, AhRR: aryl hydrocarbon receptor repressor, a.u.: arbitrary units. Pearson's r and p values corrected for age and BMI of obese subjects are indicated.

Molecular Probes, Life Technologies, Saint-Aubin, France). Nuclei were stained with 4′-6-diamidino-2-phenylindole (DAPI) to assess the monolayer integrity. The cells were examined by structured illumination microscopy using an Axio Imager 2 microscope equipped with an apotome.2 allowing optical sectioning (Zeiss, Oberkochen, Germany). Images were acquired by ZEN 2011 software (Zeiss) and analyzed using Fiji software (ImageJ 2.00-rc-69/1.52p).

2.9. Simple western blotting
Caco-2/TC7 cells were lysed as previously described [29]. Protein levels were detected in the cell lysates using a Wes capillary electrophoresis system (ProteinSimple, San José, CA, USA) according to the manufacturer's instructions. Reconstituted images and quantification were performed using Compass for SW3.1 software (ProteinSimple). Primary antibodies were rabbit anti-tricellulin (1:2000, MARVELD2 700191, Thermo Fisher Scientific) and rabbit anti-occludin (1:25, 71–1500, Thermo Fisher Scientific). Secondary antibodies and reagents used were provided in the separation and detection module kits (ProteinSimple). Junction protein levels were normalized to Hsc70 (1:100, sc7298, Santa Cruz, CliniSciences Nanterre, France).

2.10. Statistical analysis
Values were expressed as mean ± SEM. Statistical analyses were conducted using GraphPad Prism 6.0 (GraphPad Software, La Jolla, CA, USA). Two group comparisons were performed using Student's t-test (quantitative variables) or chi-squared test (categorical variables). Comparisons involving multiple groups were conducted using one-way analysis of variance (ANOVA). Pearson's correlations adjusted for age

and BMI were determined using R software (R foundation for Statistical Computing, Vienna, Austria). A level of p < 0.05 was considered significant.

3. RESULTS

3.1. Increased CD3+ T cell density in intestinal epithelium negatively correlates with expression of AhR gene targets in severe obesity
We evaluated intestinal inflammation in non-obese and subjects with severe obesity by quantifying the density of $CD3^+$ T lymphocytes in the jejunum mucosa. The epithelial to lamina propria (Epi/LP) ratio allowed quantification of the T lymphocyte recruitment in the epithelium (Figure 1A). We showed significantly higher CD3 Epi/LP ratios in the obese subjects than in the non-obese subjects (p < 0.0209). A heterogeneous distribution of CD3 Epi/LP ratios was observed within the obese cohort. To study the relevance of AhR activity in the heterogeneity of intestinal inflammation within the obese cohort, we determined the epithelial cell fraction from the same jejunum samples, the AhR expression, the well-known target genes (CYP1A1 and CYP1B1), and the recently identified AhR-target gene, IL-22 [34]. We observed strong significantly negative relationships between the AhR, CYP1A1, and IL-22 mRNA levels and CD3 Epi/LP ratios in female obese subjects (Figure 1B–D). The CYP1B1 mRNA levels and CD3 Epi/LP ratios also showed a trend (p = 0.060) toward a negative correlation (Figure 1E). However, the level of AhR repressor (AhRR) involved in the feedback regulation of AhR signaling [35] was not correlated with intestinal inflammatory cell accumulation (Figure 1F).
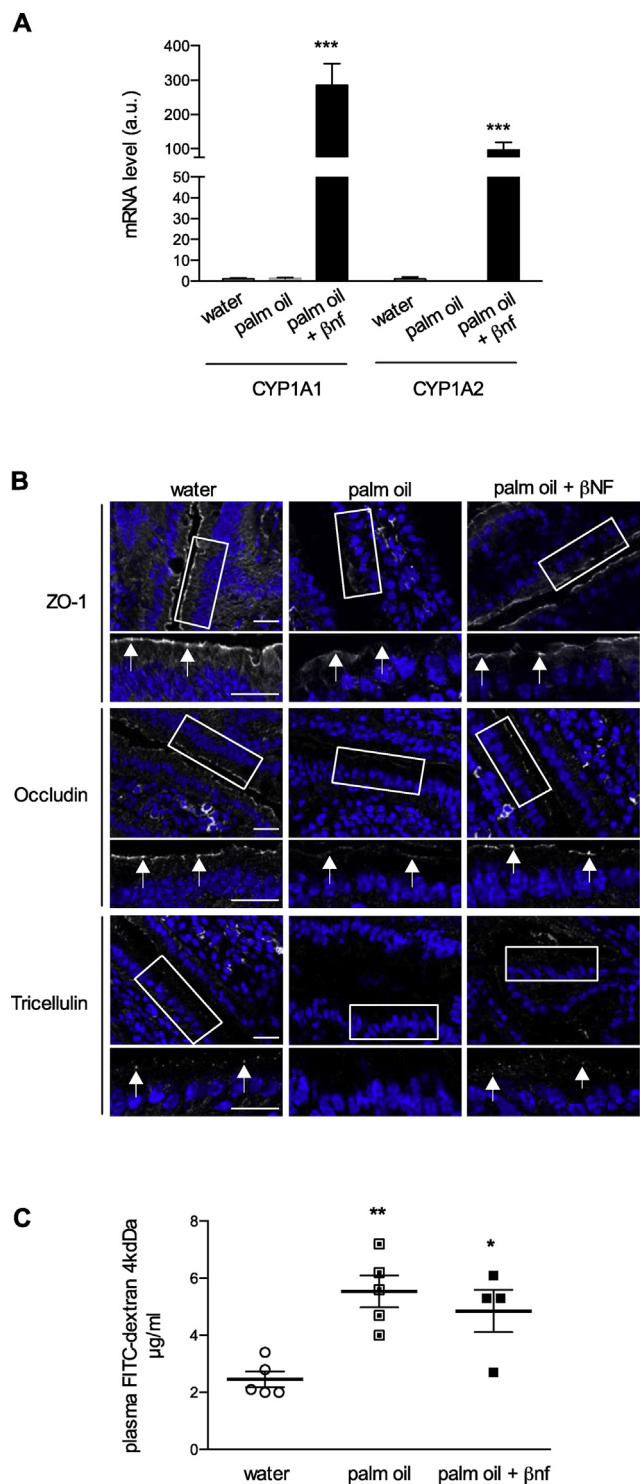
A

B

C

Figure 2: Protective role of AhR activation on cell-cell junctions in murine intestinal epithelium. Mice were submitted to 5 gavages (5x) with 200 µl water or palm oil or palm oil + βNF for five consecutive days. (**A**) The expression of CYP1A1 and CYP1A2 was determined by RT-PCR in the jejunum. Cyclophilin was used as a reference gene. The results are expressed in arbitrary units (a.u.) as the ratio of the target gene to cyclophilin (cyclo) mRNA level as mean ± SEM, n = 5, ***p < 0.001 compared to water conditions. (**B**) The distribution of tight junction proteins ZO-1, occludin, and tricellulin was analyzed by immunofluorescence on the jejunum sections. Nuclei were stained with 4′,6-diamidino-2-phenylindole (DAPI). The rectangle indicates the field used for enlargement. The white arrowheads indicate the labeling of the junction proteins. Scale bar = 20 µm. (**C**) The intestinal permeability was assessed

These results showing a negative correlation between intestinal inflammation and AhR activity in human obesity prompted us to further examine AhR activity in this context.

3.2. AhR activation protects intestinal junctional complexes during lipid load in mice

Inflammation and intestinal permeability are experimentally linked. In obesity and high-fat diet-induced models of obesity, inflammation in several tissues and endotoxemia were observed as well as low-grade systemic inflammation. All of these factors can contribute to altering intestinal permeability; in particular, circulating activated immune cells that secrete pro-inflammatory cytokines are known to alter cell-cell junctions [36]. We previously observed that 1—5 repeated gavages with palm oil in mice were sufficient to reproduce part of the events occurring in high-fat diet-induced obesity models. They induce a disruption of the intestinal barrier integrity and initiate intestinal inflammation, but without obvious systemic inflammation [11]. This short-term treatment with palm oil allowed us to obtain more direct and local effects on intestine-targeting gut permeability. We investigated the effect of AhR activation in this mouse model of lipid-induced impairment of the intestinal epithelial barrier. Mice were force fed palm oil alone or in combination with β-naphthoflavone (βNF), a potent AhR agonist (Figure 2). As expected, βNF administration markedly increased the expression of AhR target genes CYP1A1 and CYP1A2 in the jejunum (Figure 2A). Importantly, we observed that palm oil feeding impaired tight junction integrity, as shown by the loss of signal of ZO-1, occludin, and tricellulin at tight junctions (Figure 2B). The activation of AhR activity by βNF partially restored the localization of these proteins in membranes (Figure 2B). However, the administration of βNF did not prevent the increase in intestinal permeability to macromolecules (determined by measuring 4 kDa FITC-dextran) induced by palm oil (Figure 2C), suggesting that the partial restoration of cell-cell junctions was not sufficient to maintain barrier integrity. Nevertheless, these results suggest a protective role of AhR on the intestinal epithelium through direct impact on cell-cell junctions.

3.3. AhR activation prevents chemically induced damage to barrier integrity in intestinal epithelial cells

We further investigated the role of AhR on cell-cell junctions in the intestinal epithelium monolayer and examined the effect of AhR activation after barrier damage in the human intestinal epithelial Caco-2/TC7 cell line. Chemical disruption of cell-cell junctions was induced by EGTA, a calcium chelator known to alter barrier permeability [37]. We first wanted to determine whether AhR activation could prevent the loss of barrier integrity induced by EGTA (Figure 3). Caco-2/TC7 cells were treated for 4 days with βNF and EGTA was added during the last 4 h of the experiment. As expected, the treatment of Caco-2/TC7 cells with βNF increased the mRNA levels of the AhR target gene CYP1A1 (Figure 3A). While the permeability to macromolecules measured by the passage of 4 kDa FITC-dextran was increased upon chemically induced barrier damage, this increase was not modified in the presence of βNF (Figure 3B). Unexpectedly, a small increase in 4 kDa FITC-dextran flux was observed when the cells were incubated with βNF alone. We then studied the effects of AhR activation on paracellular

after the last gavage with water, palm oil, or palm oil + βNF by measuring plasma concentrations of 4 kDa FITC-dextran (FD4) 1 h after an oral FD4 load. The results are expressed in µg/ml as mean ± SEM, *p < 0.05, and **p < 0.01 compared to water. Data show one experiment representative of two independent experiments conducted with 4—5 mice in each group.
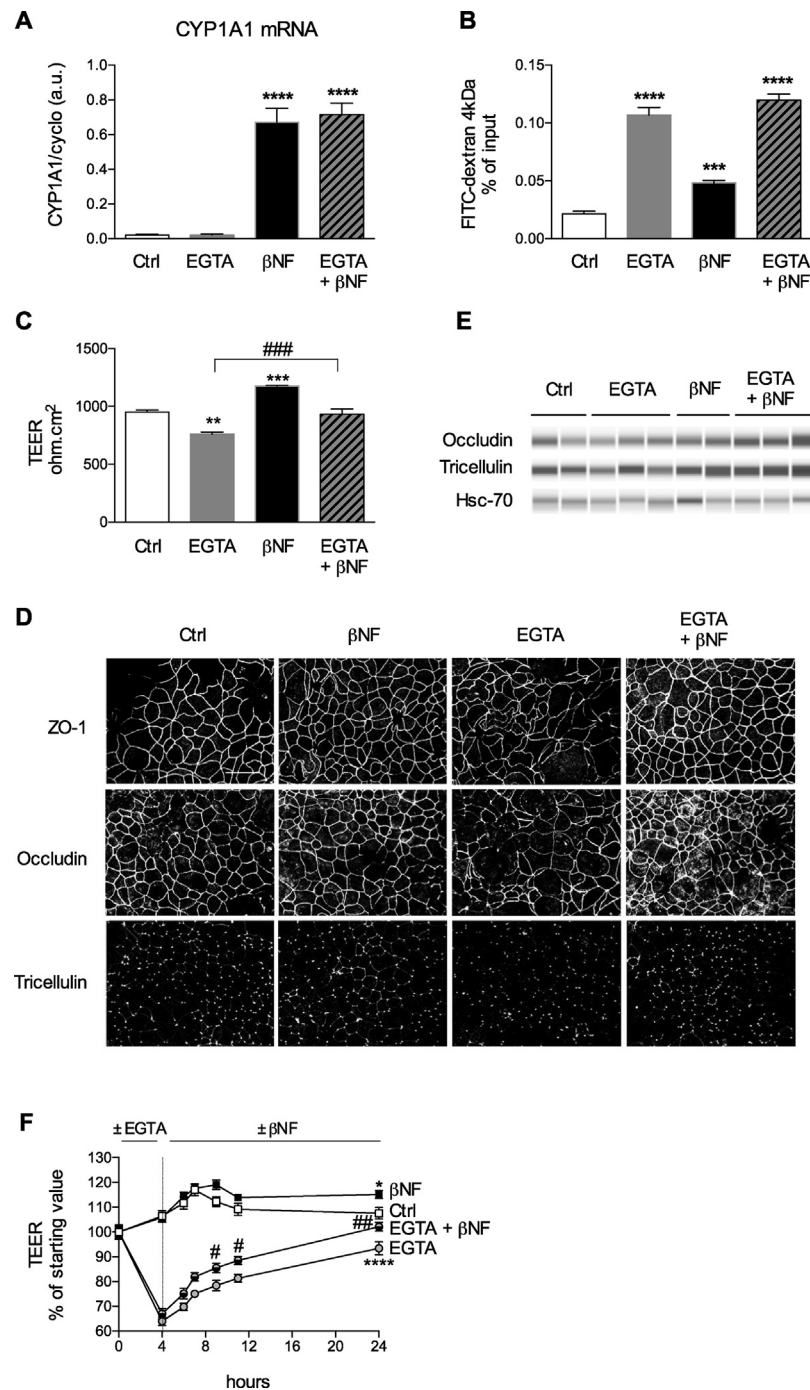
Figure 3: Protective role of AhR activation on EGTA-induced damage to barrier integrity in Caco-2/TC7 cells. (A) Caco-2/TC7 cells were pre-incubated without (Ctrl) or with 20 μM βNF for 4 consecutive days before the addition or 4.5 mM EGTA for additional 24 h βNF treatment was maintained during all of the experiments. The expression of CYP1A1 was quantified by RT-qPCR. Cyclophilin was used as a reference gene. The results are expressed in arbitrary units (a.u.) as the ratio of the target gene to cyclophilin (cyclo) mRNA level as mean $\pm$ SEM, n = 6–15 from 3 independent experiments, ****$p < 0.0001$ compared to controls. **(B)** The cells were cultured under the same conditions as in (A). Paracellular permeability across Caco-2/TC7 cell monolayers was evaluated by measuring the accumulation during 4 h of 4 kDa FITC-dextran (FD4) in the basal compartment. The results are expressed as percentage of FD4 input (amount added in the apical compartment), mean $\pm$ SEM, n = 6–15 from 3 independent experiments, ***$p < 0.001$, and ****$p < 0.0001$ compared to controls. **(C)** The cells were cultured under the same conditions as in (A). TEER was assessed in the control and treated cells. The results are expressed in ohm.cm^2 as mean $\pm$ SEM, n = 6–15 from 3 independent experiments, **$p < 0.01$, and ***$p < 0.001$ compared to controls. ###$p < 0.001$ compared to EGTA. **(D)** The cells were cultured under the same conditions as in (A). Immunofluorescence analysis was conducted to study the location of ZO-1, occludin, and tricellulin. Nuclei were stained DAPI, scale bar = 20 μm **(E)** The cells were cultured as in (A). Occludin and tricellulin protein levels were determined in cell lysates using capillary-based Western blotting. Reconstituted images are displayed. Hsc70 protein levels were used as loading controls. **(F)** Caco-2/TC7 cells were first incubated in the presence or absence of 4.5 mM EGTA for 4 h. The media were then removed and replaced by fresh media in the presence or absence of 20 μM βNF for 20 h. TEER was measured before EGTA treatment (T0), after 4 h of EGTA treatment (T4), and at different times after βNF addition. The results are expressed in percentage of TEER measured at T0 for each cell culture condition as mean $\pm$ SEM, n = 6 from 2 independent experiments. *$p < 0.05$ and ****$p < 0.0001$ compared to controls and ##$p < 0.01$ compared to EGTA.
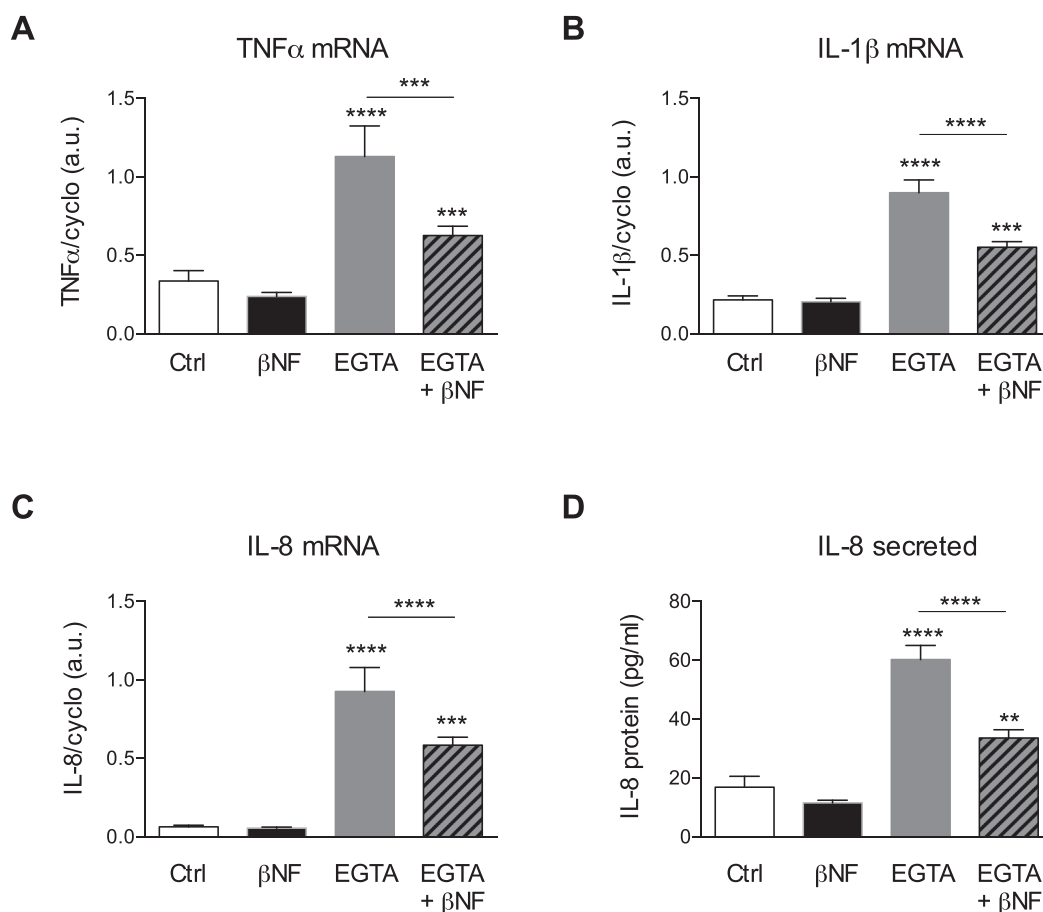
Figure 4: AhR activation prevents the increase of cytokine expression induced by EGTA. Caco-2/TC7 cells were cultured under the same conditions as in Figure 3. The mRNA levels of TNF-α (**A**), IL-1β (**B**), and IL-8 (**C**) were quantified by RT-PCR. Cyclophilin was used as a reference gene. The results are expressed in arbitrary units (a.u.) as the ratio of the target gene to cyclophilin (cyclo) mRNA level as mean ± SEM, n = 20—30. (**D**) The concentration of IL-8 protein in the basal compartment was quantified by ELISA 24 h after EGTA treatment. The results are expressed in pg/ml as mean ± SEM, n = 6. Fold increase compared to the control condition is indicated at the top of the bar plots. **p < 0.01, ***p < 0.001, and ****p < 0.0001 compared to controls unless otherwise indicated. Figure 4A,B represent data compiled for 6 independent experiments. Each experiment consisted of 3—6 independent Transwells. Figure 4C represents data compiled for 2 independent experiments conducted in triplicate.

permeability to ions measured by determining transepithelial resistance (TEER). As anticipated, chemically induced barrier damage decreased TEER, demonstrating an enhanced permeability to ions (Figure 3C). We showed that βNF prevented chemically induced barrier damage by maintaining TEER at control values. TEER reinforcement was also noticed when the cells were incubated with βNF alone. We used immunofluorescence and Western blotting to analyze the localization and expression of the tight junction proteins ZO-1, occludin, and tricellulin in cells pretreated or not with βNF under chemically induced barrier damage conditions. We observed strong tight junction disorganization accompanied by a decrease in fluorescence intensity and mislocalization of these proteins upon chemically induced barrier damage, which was prevented by βNF. No obvious effect was observed in the presence of βNF alone (Figure 3D). An increase in protein levels of occludin and tricellulin was observed in the presence of βNF alone and upon chemically induced barrier damage in βNF-treated cells (Figure 3E). These results indicated that pretreatment with the AhR agonist βNF prevents chemically induced damage to the intestinal epithelium monolayer by a mechanism involving an increase in the levels of occludin and tricellulin proteins and their localization at cell—cell contacts.

We then determined whether the activation of AhR could ameliorate the recovery of normal permeability after chemically induced damage. We incubated the cells for 4 h with EGTA and then added new culture medium containing or not the AhR agonist (Figure 3F). We showed that the addition of βNF improved the recovery of TEER after chemically induced barrier damage. This amelioration was apparently initiated in the first hours after βNF addition and reached statistical significance after 5 h.

Altogether, the results from the *in vitro* experiments showed that the activation of AhR preserved and restored the intestinal epithelial cell monolayer from damage provoked by disruption of cell-cell junctions.

3.4. AhR activation prevents the increase in cytokine expression associated with epithelium damage

Intestinal epithelial cells can produce many cytokines and chemokines [38,39]. The CXCL8 (IL-8), TNFA, and IL1B genes showed high expression in the intestinal Caco-2/TC7 cell model. We previously showed in this model that chemically induced barrier damage provoked an increase in the expression of TNFα, IL1-β, and IL-8 and the secretion of IL-8 [11]. We determined whether the presence of the AhR agonist counteracted these effects. Whereas barrier damage was
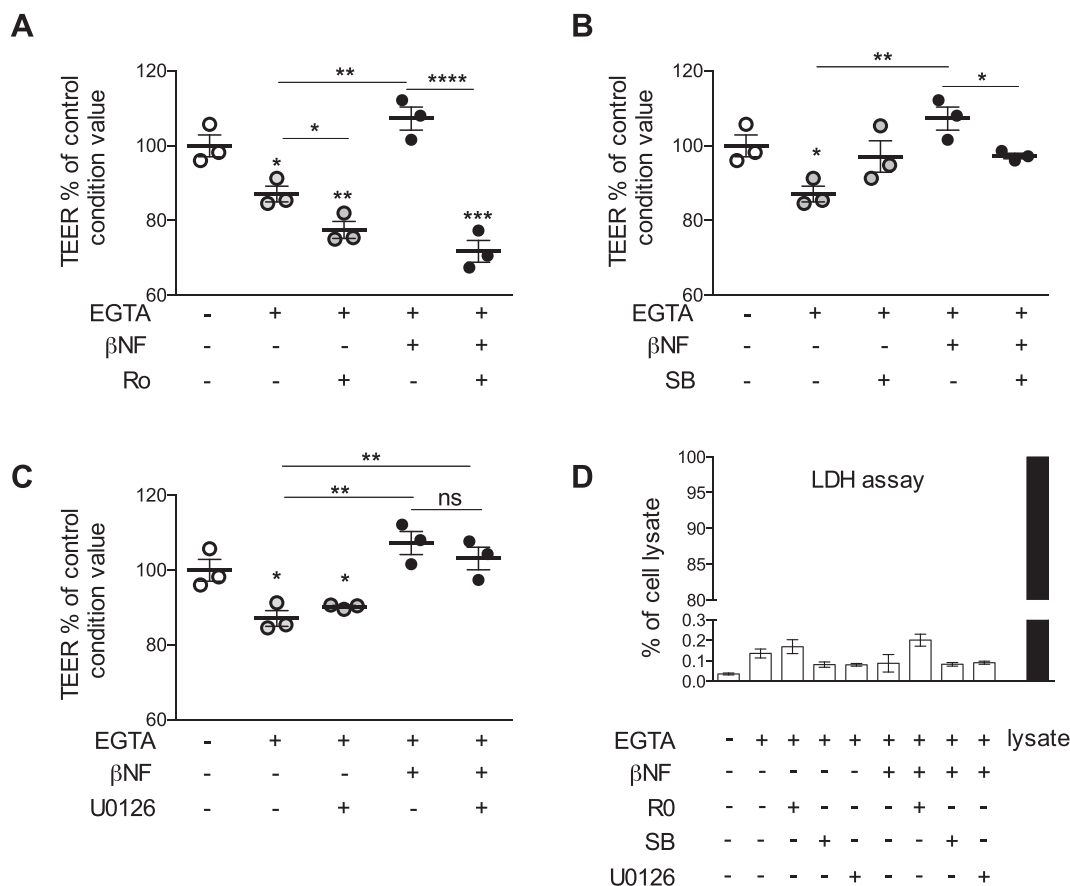
Figure 5: **Signaling pathways are involved in the preventive effect of AhR activation on transepithelial resistance.** Caco-2/TC7 cells were pre-incubated with (**A**) 5 μM of protein kinase C inhibitor Ro 31—8220 (Ro), (**B**) 20 μM of p38MAPK inhibitor SB203580 (SB), or (**C**) 10 μM of protein kinase ERK1/2 inhibitor U0126 1 h prior βNF addition. These treatments were repeated daily for 4 days. EGTA was added for the last 4 h of treatment. Transepithelial resistance (TEER) was measured at the end of the experiment. The results are expressed in percentage of TEER value measured in control conditions at the end of the experiment as mean ± SEM, n = 3. *p < 0.05, **p < 0.01, ***p < 0.001, and ****p < 0.0001 compared to controls unless otherwise indicated. Data are representative of 2 independent experiments conducted in triplicate. (**D**) Lactate dehydrogenase (LDH) was quantified in the apical medium and the results are expressed as percentage of LDH activity measured in the total cell lysate (mean ± SEM), n = 6.

significant, pretreatment with βNF prevented the increase in the mRNA levels of the three investigated cytokines (Figure 4A—C) and the secretion of IL-8 in the basal medium (Figure 4D). These results showed that *in vitro* activation of AhR precludes the inflammatory response of intestinal epithelial cells during chemical injury of the epithelial barrier.

3.5. AhR activation exerts its preventive effect through the PKC and p38MAPK signaling pathways

The assembly and maintenance of cell-cell junctions and in particular tight junctions are controlled and regulated by phosphorylation/dephosphorylation processes [40] involving regulatory proteins such as kinases or phosphatases [41—43]. We investigated the impact of these signaling pathways on the protective effect of AhR activation on the EGTA-dependent decrease in TEER in Caco-2/TC7 cells. The cells were pre-incubated and then treated daily for 4 consecutive days with specific inhibitors of protein kinases C (Ro 318220), p38MAP kinase (SB203580), or ERK1/2 (U0126) 1 h before the addition of βNF. Chemical barrier damage was induced for the last 4 h of treatment. We confirmed that barrier damage was associated with a decrease in TEER that was counteracted in the presence of AhR agonist. We further showed that the maintenance of TEER by βNF treatment in barrier-damaged cell monolayers did not occur when the cells were

pretreated with Ro 31-8220 (Figure 5A) or SB203580 (Figure 5B). However, in the absence of βNF treatment, we found a decrease in TEER in the presence of Ro 31-8220 in chemically damaged epithelial barriers (Figure 5A), indicating that the inhibition of protein kinase C was sufficient to modify TEER. As Ro 31-8220 can also inhibit protein kinase A and GSK3β, we cannot exclude the participation of these protein kinases in the effects of βNF. Contrary to the effects of PKC and p38MAPK inhibitors, the inhibition of protein kinase ERK1/2 by U0126 treatment did not block the βNF-dependent maintenance of TEER to the control value (Figure 5C). No toxic effect of treatments (assessed by measuring lactate dehydrogenase release in the medium) was observed (Figure 5D).

These results suggest a potential implication of PKC and p38MAPK in the protective effect of βNF on intestinal permeability to ions (TEER).

4. DISCUSSION

Combining human studies, mouse *in vivo* investigations, and a cell culture model of human enterocytes, we showed that the transcriptional factor AhR is an important contributor to intestinal barrier maintenance (Figure 6).

We demonstrated a negative correlation between the expression of AhR target genes and inflammation in jejunum samples from subjects
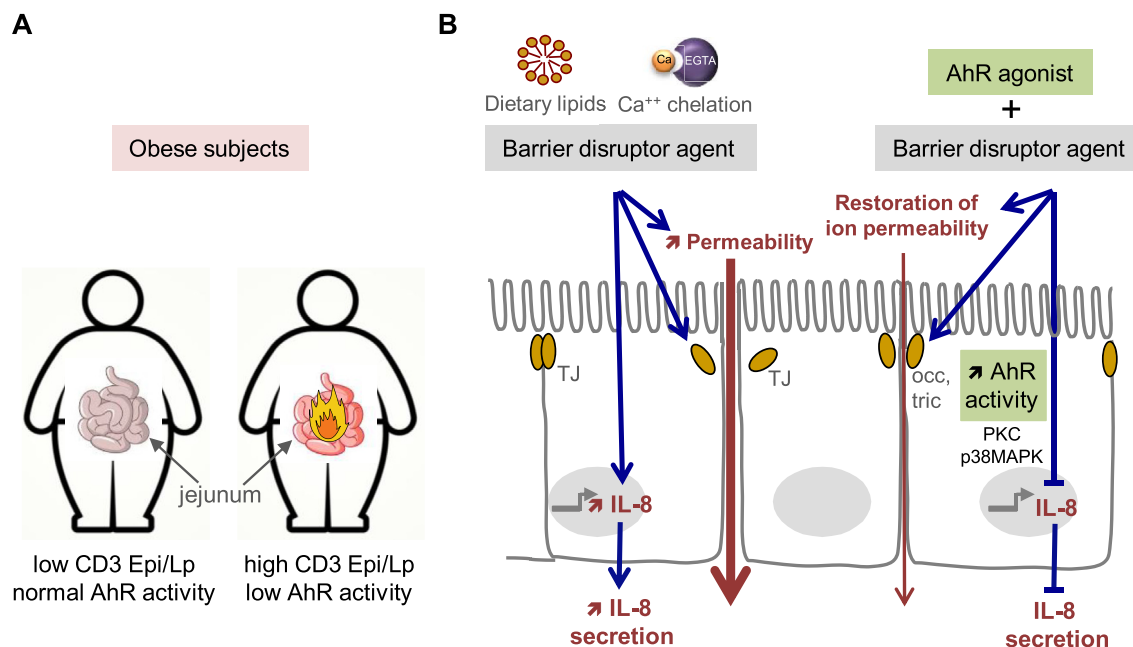
Figure 6: Protective role of AhR on intestinal barrier and cytokine expression. (A) Obese non-diabetic subjects were classified according to their small intestinal inflammation score established by the densities of T lymphocytes using the CD3 marker. The epithelium/lamina propria (Epi/Lp) CD3 ratio quantified T lymphocyte infiltration within the epithelium in the jejunum samples. Obese subjects with high CD3 Epi/Lp ratios displayed lower AhR activity. **(B)** In the intestinal epithelial cells, lipid load or treatment with calcium chelator (EGTA) damaged barrier integrity (increase in paracellular permeability and alteration of tight junctions) and induced the expression and secretion of pro-inflammatory cytokine IL-8. In the human intestinal epithelial Caco-2/TC7 cell line, the activation of AhR by an agonist increased the expression of occludin (occ) and tricellulin (tric) and improved their localization at tight junctions (TJ), restored paracellular permeability to ions, and prevented the IL-8 expression and secretion induced by barrier disruptor agent through mechanisms involving protein kinases C and p38MAPK.

with obesity. This observation suggests that low AhR activity is linked to low-grade inflammation in human obesity. This potential decrease of AhR tone in obesity may be related to several mediators, including changes in gut microbiota composition. It was reported that endogenous AhR ligands are produced by intestinal bacteria by metabolizing nutrients such as tryptophan and butyrate, a short-chain fatty acid that can activate the intestinal AhR tone [44]. Intestinal inflammation and changes in fecal microbiota composition of subjects suffering from intestinal bowel diseases were associated with low levels of fecal AhR ligands [16]. Diet supplementation with *Lactobacillus* strains, which display a high natural capacity to produce AhR ligands, improved the metabolic impairment induced by high-fat diets [24,45] or reduced the severity of chemically induced colitis in mice [16]. However, obesity is often associated with an increased fecal abundance of *Lactobacillus* species [46—48], and it is unclear whether this change in abundance is accompanied by an increase in the function of this bacterial species. Indeed, low levels of AhR ligands in feces were correlated with high corpulence in humans [24]. Moreover, *Lactobacillus* strain administration showed beneficial effects, albeit moderate, on fat mass reduction in obesity [45]. The mechanisms involved in these effects require elucidation.

We demonstrated that AhR activation prevented the increase in cytokine expression induced by chemical treatment disrupting cell-cell junctions. Several mechanisms are involved in the expression of cytokines in immune cells, most linked to the activation of NF-kB pathways and protein kinases; however, little is known about those specifically responsible for the expression of cytokines by intestinal epithelial cells [49]. We provided mechanistic information regarding the link between AhR activation and intestinal barrier properties. We showed in mice submitted to a lipid load or human intestinal

epithelial cell line that AhR activation by the agonist βNF preserved the integrity of the intestinal epithelium by maintaining paracellular permeability to ions and preserving cell-cell junctions. Experimental approaches using Caco-2/TC7 cells revealed increased occludin and tricellulin protein levels after βNF treatment. Experimental approaches using Caco-2/TC7 cells demonstrated that AhR agonist protects epithelial cells from the deleterious effects of treatment that specifically targets cell-cell junctions (EGTA), complementary to recent reports showing a protective role of AhR on the intestinal barrier under inflammatory conditions or in the presence of LPS [17,18,50]. In addition to a preserved localization at tight junctions, increased global protein levels of occludin and tricellulin were observed after βNF treatment. AhR is a transcription factor known to bind specific responsive elements in the promoter of its target genes [51]. To date, no AhR-responsive elements have been described on the promoter of occludin and tricellulin genes, suggesting that the effects of AhR occur through indirect pathways. In this context, our study revealed the potential implication of protein kinase C and p38MAPK in the protective effect of AhR activity on paracellular permeability. Numerous observations indicated that AhR triggers several cellular pathways via the activation of protein kinases or its E3 ubiquitin protein ligase activity [15,52]. Studies suggested that Src tyrosine kinase is a member of the multiprotein AhR complex localized in the cytosol in the absence of AhR ligands. The interaction of AhR with its ligands provokes the dissociation of this complex, the release and activation of Src kinase, and the translocation of AhR in the nucleus [15]. Interestingly, Src kinase is also involved in the maintenance of tight junctions [53]. Other crosstalk between AhR signaling and mechanisms controlling paracellular permeability such as phosphorylation/dephosphorylation or tight junction protein

stabilization processes [54—56] can be considered. Indeed, it has been observed that PKC and protein Par-6 are members of a multiprotein complex involved in the maintenance of cell polarity [54] and Par-6 is also involved in the protective effects of AhR on the intestinal epithelial barrier [18]. Further studies are required to fully understand the mechanisms involved in the protective effects of AhR on the intestinal epithelium.

5. CONCLUSION

Our study demonstrated an important protective role of AhR on intestinal barrier integrity including preserved cell-cell junctions and downregulation of inflammatory markers. This indicates that in obesity, this integrity might be altered through an imbalance between AhR tone and low-grade inflammation. Lower intestinal AhR activity may thus contribute to local and systemic inflammation through a loss of intestinal barrier integrity in obesity. AhR agonist administration via food or drugs constitutes a therapeutic strategy to protect intestinal functions in metabolic diseases.

AUTHOR CONTRIBUTIONS

B.G.P, S.G., and V.C. designed and conducted the experiments and analyzed the data. D.A. acquired the tight junction images using apotome and analyzed these proteins with simple Western blotting. K.G., S.A., and E.B.L. conducted CD3 labeling and quantification on the human jejunum samples. H.S. conducted the statistical analyses. C.P. and K.C. coordinated the clinical investigation. L.G. performed the patient surgery. C.P. and K.C. contributed to subject recruitment, patient phenotyping, and sample collection. V.C. wrote the paper. B.G.P., C.P., K.C., H.S., D.A., and A.L. revised the manuscript versions. All of the authors reviewed the results and approved the final version of the manuscript.

CONFLICT OF INTEREST

The authors declare no conflicts of interest.

REFERENCES

[1] Stolarczyk, E., 2017. Adipose tissue inflammation in obesity: a metabolic or immune response? Current Opinion in Pharmacology 37:35—40.

[2] Reilly, S.M., Saltiel, A.R., 2017. Adapting to obesity with adipose tissue inflammation. Nature Reviews Endocrinology 13(11):633—643.

[3] Loomis, A.K., Kabadi, S., Preiss, D., Hyde, C., Bonato, V., St Louis, M., et al., 2016. Body mass index and risk of nonalcoholic fatty liver disease: two electronic health record prospective studies. Journal of Clinical Endocrinology & Metabolism 101(3):945—952.

[4] Monteiro-Sepulveda, M., Touch, S., Mendes-Sa, C., Andre, S., Poitou, C., Allatif, O., et al., 2015. Jejunal T cell inflammation in human obesity correlates with decreased enterocyte insulin signaling. Cell Metabolism 22(1):113—124.

[5] Makki, K., Froguel, P., Wolowczuk, I., 2013. Adipose tissue in obesity-related inflammation and insulin resistance: cells, cytokines, and chemokines. ISRN Inflammation 2013:139239.

[6] Cani, P.D., Bibiloni, R., Knauf, C., Waget, A., Neyrinck, A.M., Delzenne, N.M., et al., 2008. Changes in gut microbiota control metabolic endotoxemia-induced inflammation in high-fat diet-induced obesity and diabetes in mice. Diabetes 57(6):1470—1481.

[7] Cani, P.D., Amar, J., Iglesias, M.A., Poggi, M., Knauf, C., Bastelica, D., et al., 2007. Metabolic endotoxemia initiates obesity and insulin resistance. Diabetes 56(7):1761—1772.

[8] Araujo, J.R., Tomas, J., Brenner, C., Sansonetti, P.J., 2017. Impact of high-fat diet on the intestinal microbiota and small intestinal physiology before and after the onset of obesity. Biochimie 141:97—106.

[9] Johnson, A.M., Costanzo, A., Gareau, M.G., Armando, A.M., Quehenberger, O., Jameson, J.M., et al., 2015. High fat diet causes depletion of intestinal eosinophils associated with intestinal permeability. PloS One 10(4):e0122195.

[10] Hamilton, M.K., Boudry, G., Lemay, D.G., Raybould, H.E., 2015. Changes in intestinal barrier function and gut microbiota in high-fat diet-fed rats are dynamic and region dependent. American Journal of Physiology - Gastrointestinal and Liver Physiology 308(10):G840—G851.

[11] Ghezzal, S., Postal, B.G., Quevrain, E., Brot, L., Seksik, P., Leturque, A., et al., 2020. Palmitic acid damages gut epithelium integrity and initiates inflammatory cytokine production. Biochimica et Biophysica Acta (BBA) - Molecular and Cell Biology of Lipids 1865(2):158530.

[12] Genser, L., Aguanno, D., Soula, H.A., Dong, L., Trystram, L., Assmann, K., et al., 2018. Increased jejunal permeability in human obesity is revealed by a lipid challenge and is linked to inflammation and type 2 diabetes. The Journal of Pathology.

[13] Kawajiri, K., Fujii-Kuriyama, Y., 2017. The aryl hydrocarbon receptor: a multifunctional chemical sensor for host defense and homeostatic maintenance. Experimental Animals 66(2):75—89.

[14] Ramadoss, P., Marcus, C., Perdew, G.H., 2005. Role of the aryl hydrocarbon receptor in drug metabolism. Expert Opinion on Drug Metabolism and Toxicology 1(1):9—21.

[15] Rothhammer, V., Quintana, F.J., 2019. The aryl hydrocarbon receptor: an environmental sensor integrating immune responses in health and disease. Nature Reviews Immunology 19(3):184—197.

[16] Lamas, B., Richard, M.L., Leducq, V., Pham, H.P., Michel, M.L., Da Costa, G., et al., 2016. CARD9 impacts colitis by altering gut microbiota metabolism of tryptophan into aryl hydrocarbon receptor ligands. Nature Medicine 22(6):598—605.

[17] Yu, M., Wang, Q., Ma, Y., Li, L., Yu, K., Zhang, Z., et al., 2018. Aryl hydrocarbon receptor activation modulates intestinal epithelial barrier function by maintaining tight junction integrity. International Journal of Biological Sciences 14(1):69—77.

[18] Yu, K., Ma, Y., Zhang, Z., Fan, X., Li, T., Li, L., et al., 2018. AhR activation protects intestinal epithelial barrier function through regulation of Par-6. Journal of Molecular Histology 49(5):449—458.

[19] Xu, C.X., Wang, C., Zhang, Z.M., Jaeger, C.D., Krager, S.L., Bottum, K.M., et al., 2015. Aryl hydrocarbon receptor deficiency protects mice from diet-induced adiposity and metabolic disorders through increased energy expenditure. International Journal of Obesity 39(8):1300—1309.

[20] Moyer, B.J., Rojas, I.Y., Kerley-Hamilton, J.S., Nemani, K.V., Trask, H.W., Ringelberg, C.S., et al., 2017. Obesity and fatty liver are prevented by inhibition of the aryl hydrocarbon receptor in both female and male mice. Nutrition Research 44:38—50.

[21] Lee, J.H., Wada, T., Febbraio, M., He, J., Matsubara, T., Lee, M.J., et al., 2010. A novel role for the dioxin receptor in fatty acid metabolism and hepatic steatosis. Gastroenterology 139(2):653—663.

[22] He, J., Hu, B., Shi, X., Weidert, E.R., Lu, P., Xu, M., et al., 2013. Activation of the aryl hydrocarbon receptor sensitizes mice to nonalcoholic steatohepatitis by deactivating mitochondrial sirtuin deacetylase Sirt3. Molecular and Cellular Biology 33(10):2047—2055.

[23] Wada, T., Sunaga, H., Miyata, K., Shirasaki, H., Uchiyama, Y., Shimba, S., 2016. Aryl hydrocarbon receptor plays protective roles against high fat diet (HFD)-induced hepatic steatosis and the subsequent lipotoxicity via direct transcriptional regulation of Socs3 gene expression. Journal of Biological Chemistry 291(13):7004—7016.

[24] Natividad, J.M., Agus, A., Planchais, J., Lamas, B., Jarry, A.C., Martin, R., et al., 2018. Impaired aryl hydrocarbon receptor ligand production by the gut microbiota is a key factor in metabolic syndrome. Cell Metabolism 28(5):737—749 e734.

[25] Aron-Wisnewsky, J., Prifti, E., Belda, E., Ichou, F., Kayser, B.D., Dao, M.C., et al., 2019. Major microbiota dysbiosis in severe obesity: fate after bariatric surgery. Gut 68(1):70—82.

[26] Dalmas, E., Rouault, C., Abdennour, M., Rovere, C., Rizkalla, S., Bar-Hen, A., et al., 2011. Variations in circulating inflammatory factors are related to changes in calorie and carbohydrate intakes early in the course of surgery-induced weight reduction. American Journal of Clinical Nutrition 94(2):450—458.

[27] Chantret, I., Rodolosse, A., Barbat, A., Dussaulx, E., Brot-Laroche, E., Zweibaum, A., et al., 1994. Differential expression of sucrase-isomaltase in clones isolated from early and late passages of the cell line Caco-2: evidence for glucose-dependent negative regulation. Journal of Cell Science 107(Pt 1):213—225.

[28] Morel, E., Ghezzal, S., Lucchi, G., Truntzer, C., Pais de Barros, J.P., Simon-Plas, F., et al., 2018. Cholesterol trafficking and raft-like membrane domain composition mediate scavenger receptor class B type 1-dependent lipid sensing in intestinal epithelial cells. Biochimica et Biophysica Acta 1863(2):199—211.

[29] Beaslas, O., Cueille, C., Delers, F., Chateau, D., Chambaz, J., Rousset, M., et al., 2009. Sensing of dietary lipids by enterocytes: a new role for SR-BI/CLA-1. PloS One 4(1):e4278.

[30] Petit, C.S., Barreau, F., Besnier, L., Gandille, P., Riveau, B., Chateau, D., et al., 2012. Requirement of cellular prion protein for intestinal barrier function and mislocalization in patients with inflammatory bowel disease. Gastroenterology 143(1):122—132 e115.

[31] Ikenouchi, J., Sasaki, H., Tsukita, S., Furuse, M., Tsukita, S., 2008. Loss of occludin affects tricellular localization of tricellulin. Molecular Biology of the Cell 19(11):4687—4693.

[32] Ikenouchi, J., Furuse, M., Furuse, K., Sasaki, H., Tsukita, S., Tsukita, S., 2005. Tricellulin constitutes a novel barrier at tricellular contacts of epithelial cells. The Journal of Cell Biology 171(6):939—945.

[33] Saitou, M., Ando-Akatsuka, Y., Itoh, M., Furuse, M., Inazawa, J., Fujimoto, K., et al., 1997. Mammalian occludin in epithelial cells: its expression and sub-cellular distribution. European Journal of Cell Biology 73(3):222—231.

[34] Parks, O.B., Pociask, D.A., Hodzic, Z., Kolls, J.K., Good, M., 2015. Interleukin-22 signaling in the regulation of intestinal health and disease. Frontiers in Cellular Developmental Biology 3:85.

[35] Vogel, C.F.A., Haarmann-Stemmann, T., 2017. The aryl hydrocarbon receptor repressor - more than a simple feedback inhibitor of AhR signaling: clues for its role in inflammation and cancer. Current Opinion in Toxicology 2:109—119.

[36] Duan, Y., Zeng, L., Zheng, C., Song, B., Li, F., Kong, X., et al., 2018. Inflammatory links between high fat diets and diseases. Frontiers in Immunology 9:2649.

[37] Rothen-Rutishauser, B., Riesen, F.K., Braun, A., Gunthert, M., Wunderli-Allenspach, H., 2002. Dynamics of tight and adherens junctions under EGTA treatment. Journal of Membrane Biology 188(2):151—162.

[38] Stadnyk, A.W., 2002. Intestinal epithelial cells as a source of inflammatory cytokines and chemokines. Canadian Journal of Gastroenterology 16(4):241—246.

[39] Miron, N., Cristea, V., 2012. Enterocytes: active cells in tolerance to food and microbial antigens in the gut. Clinical and Experimental Immunology 167(3):405—412.

[40] Garcia, M.A., Nelson, W.J., Chavez, N., 2018. Cell-cell junctions organize structural and signaling networks. Cold Spring Harbor Perspectives in Biology 10(4).

[41] Stein, J., Kottra, G., 1997. [Intestinal intercellular tight junctions. I. Structure and molecular mechanisms of regulation]. Zeitschrift für Gastroenterologie 35(3):205—220.

[42] Mitic, L.L., Anderson, J.M., 1998. Molecular architecture of tight junctions. Annual Review of Physiology 60:121—142.

[43] Matter, K., Balda, M.S., 2003. Signalling to and from tight junctions. Nature Reviews Molecular Cell Biology 4(3):225—236.

[44] Marinelli, L., Martin-Gallausiaux, C., Bourhis, J.M., Beguet-Crespel, F., Blottiere, H.M., Lapaque, N., 2019. Identification of the novel role of butyrate as AhR ligand in human intestinal epithelial cells. Scientific Reports 9(1):643.

[45] Kang, Y., Cai, Y., 2018. The development of probiotics therapy to obesity: a therapy that has gained considerable momentum. Hormones 17(2):141—151.

[46] Peters, B.A., Shapiro, J.A., Church, T.R., Miller, G., Trinh-Shevrin, C., Yuen, E., et al., 2018. A taxonomic signature of obesity in a large study of American adults. Scientific Reports 8(1):9749.

[47] Million, M., Maraninchi, M., Henry, M., Armougom, F., Richet, H., Carrieri, P., et al., 2012. Obesity-associated gut microbiota is enriched in Lactobacillus reuteri and depleted in Bifidobacterium animalis and Methanobrevibacter smithii. International Journal of Obesity 36(6):817—825.

[48] Armougom, F., Henry, M., Vialettes, B., Raccah, D., Raoult, D., 2009. Monitoring bacterial community of human gut microbiota reveals an increase in Lactobacillus in obese patients and Methanogens in anorexic patients. PloS One 4(9):e7125.

[49] Andrews, C., McLean, M.H., Durum, S.K., 2018. Cytokine tuning of intestinal epithelial function. Frontiers in Immunology 9:1270.

[50] Singh, R., Chandrashekharappa, S., Bodduluri, S.R., Baby, B.V., Hegde, B., Kotla, N.G., et al., 2019. Enhancement of the gut barrier integrity by a microbial metabolite through the Nrf2 pathway. Nature Communications 10(1):89.

[51] Guyot, E., Chevallier, A., Barouki, R., Coumoul, X., 2013. The AhR twist: ligand-dependent AhR signaling and pharmaco-toxicological implications. Drug Discovery Today 18(9—10):479—486.

[52] Larigot, L., Juricek, L., Dairou, J., Coumoul, X., 2018. AhR signaling pathways and regulatory functions. Biochimie Open 7:1—9.

[53] Dorfel, M.J., Huber, O., 2012. Modulation of tight junction structure and function by kinases and phosphatases targeting occludin. Journal of Biomedicine and Biotechnology, 807356, 2012.

[54] Schuhmacher, D., Sontag, J.M., Sontag, E., 2019. Protein phosphatase 2A: more than a passenger in the regulation of epithelial cell-cell junctions. Frontiers in Cellular Developmental Biology 7:30.

[55] Turner, J.R., 2009. Intestinal mucosal barrier function in health and disease. Nature Reviews Immunology 9(11):799—809.

[56] Van Itallie, C.M., Anderson, J.M., 2018. Phosphorylation of tight junction transmembrane proteins: many sites, much to do. Tissue Barriers 6(1): e1382671.

12   MOLECULAR METABOLISM 39 (2020) 101007

www.molecularmetabolism.com